Draft version February 25, 2024
Preprint typeset using LaTeX style emulateapj v. 11/10/09

arXiv:1111.1791v1 [astro-ph.SR] 8 Nov 2011

THEORETICAL CEPHEID PERIOD-LUMINOSITY AND PERIOD-COLOR RELATIONS IN *SPITZER* IRAC BANDS

Chow-Choong Ngeow
Graduate Institute of Astronomy, National Central University, Jhongli City, 32001, Taiwan

Marcella Marconi
Osservatorio Astronomico di Capodimonte, Via Moiariello 16, 80131 Napoli, Italy

Ilaria Musella
Osservatorio Astronomico di Capodimonte, Via Moiariello 16, 80131 Napoli, Italy

Michele Cignoni
Department of Astronomy, Bologna University, via Ranzani 1, 40127 Bologna, Italy

and

Shashi M. Kanbur
Department of Physics, State University of New York at Oswego, Oswego, NY 13126, USA

Draft version February 25, 2024

ABSTRACT

In this paper the synthetic period-luminosity (P-L) relations in *Spitzer's* IRAC bands, based on a series of theoretical pulsation models with varying metal and helium abundance, were investigated. Selected sets of these synthetic P-L relations were compared to the empirical IRAC band P-L relations recently determined from Galactic and Magellanic Clouds Cepheids. For the Galactic case, synthetic P-L relations from model sets with ($Y = 0.26$, $Z = 0.01$), ($Y = 0.26$, $Z = 0.02$) and ($Y = 0.28$, $Z = 0.02$) agree with the empirical Galactic P-L relations derived from the *Hubble Space Telescope* parallaxes. For Magellanic Cloud Cepheids, the synthetic P-L relations from model sets with ($Y = 0.25$, $Z = 0.008$) agree with both of the empirical Large Magellanic Cloud (LMC) and Small Magellanic Cloud (SMC) P-L relations. Analysis of the synthetic P-L relations from all model sets suggested that the IRAC band P-L relations may not be independent of metallicity, as the P-L slopes and intercepts could be affected by the metallicity and/or helium abundance. We also derive the synthetic period-color (P-C) relations in the IRAC bands. Non-vanishing synthetic P-C relations were found for certain combinations of IRAC band filters and metallicity. However, the synthetic P-C relations disagreed with the $[3.6]-[8.0]$ P-C relation recently found for the Galactic Cepheids. The synthetic $[3.6]-[4.5]$ P-C slope from ($Y = 0.25$, $Z = 0.008$) model set, on the other hand, is in excellent agreement to the empirical LMC P-C counterpart, if a period range of $1.0 < \log(P) < 1.8$ is adopted.

Subject headings: distance scale — stars: variables: Cepheids

1. INTRODUCTION

The mid-infrared Cepheid period-luminosity (P-L, also known as the Leavitt Law) relation will be important in the *James Webb Space Telescope* (*JWST*) era, as it holds the promise of deriving the Hubble constant at the $\sim 2\%$ level (Freedman & Madore 2010; Freedman et al. 2011). Motivated by this, the *Spitzer's* IRAC band (3.6μm, 4.5μm, 5.8μm and 8.0μm) P-L relations were derived for Cepheids in our Galaxy (Marengo et al. 2010), in the Large Magellanic Cloud (LMC, Freedman et al. 2008; Ngeow & Kanbur 2008; Madore et al. 2009; Ngeow et al. 2009; Scowcroft et al. 2011), and in the Small Magellanic Cloud (SMC; Ngeow & Kanbur 2010).

The slopes of the IRAC band P-L relations are expected to be insensitive to metallicity (Freedman et al. 2008; Freedman & Madore 2010; Freedman et al. 2011). The empirical slopes derived from a small number of Galactic Cepheids that possess parallax distances (Marengo et al. 2010), and the Magellanic Cloud Cepheids based on the OGLE-III data (see Ngeow et al. 2009; Ngeow & Kanbur 2010, for more details) are all consistent with each other. However, these slopes do not agree with the slopes derived from Galactic Cepheids that are based on the infrared surface brightness (IRSB) method (Marengo et al. 2010) and from a smaller number of LMC Cepheids (Madore et al. 2009). Therefore, the aim of this paper is to compare these empirical P-L relations to the synthetic IRAC band P-L relations based on a series of theoretical pulsating models at various metallicities, and investigate the sensitivity of IRAC band PL relations to metallicity.

Brief description of the pulsation models is given in the next section, and the synthetic P-L relations based on these models are presented in Section 3. We compared these synthetic P-L relations to their empirical counterparts and investigated the possible metallicity dependence of the synthetic IRAC band P-L relations in Sections 4 and 5, respectively. In Section 6, synthetic period-color (P-C) relations in the IRAC bands were also

derived. Discussion and conclusion are presented in Section 7.

2. THE PULSATIONAL MODELS

The synthetic P-L relations adopted in this paper are based on extensive and detailed sets of nonlinear, pulsation models including a non-local, time-dependent treatment of the coupling between pulsation and convection. These models allow us to predict not only the periods and the blue boundary of the instability strip, but also the pulsation amplitudes, the detailed light and radial velocity curve morphology, and the complete topology of the strip, including the red edge (Bono et al. 1999; Fiorentino et al. 2002; Marconi et al. 2005, 2010). For each chemical composition and mass, an evolutionary mass-luminosity (M-L) relation was adopted (see Marconi et al. 2005, for details) and a wide range of effective temperature was explored. We note that even if the effect of varying the M-L relations has been investigated for specific chemical compositions (see, for examples, Bono et al. 1999, 2000; Caputo et al. 2005) in this analysis we assume for all the chemical composition a canonical M-L relation, neglecting both mass loss and overshooting during the previous H burning phase. This is a limitation of the adopted model sets as the above mentioned phenomena affect the P-L relations and the corresponding distance determinations (see Section 7). In total, 17 sets of model with varying helium (Y) and metal (Z) abundance are considered in this paper, most of them are the same model sets presented in Bono et al. (2010).

From the resulting theoretical instability strips and the relations connecting the periods to the intrinsic stellar parameters, synthetic P-L relations have been constructed. To this purpose, we populated the predicted instability strip by adopting the procedure suggested by Kennicutt et al. (1998). In particular, $\sim$ 1000 pulsators were uniformly distributed from the blue to the red boundary of the instability strip, with a mass law as given by $\mathrm{d}n/\mathrm{d}m = m^{-3}$ over the mass range 5 - 11$M_{\odot}$ (see Caputo et al. 2000, for further details). In order to translate the pulsational properties of the investigated Cepheid models in the *Spitzer* IRAC bands, we have directly convolved the predicted bolometric light curves with the *Spitzer* filter profiles using the general integral equation (see, for example, Girardi et al. 2002):

$$m_{S_\lambda} = -2.5 \log \left(\frac{\int_{\lambda_1}^{\lambda_2} \lambda f_\lambda S_\lambda \mathrm{d}\lambda}{\int_{\lambda_1}^{\lambda_2} \lambda f_\lambda^0 S_\lambda \mathrm{d}\lambda} \right) \quad (1)$$

where S_λ is the IRAC Spectral Response Curve[1], f_λ is the stellar flux (that corresponds to model atmospheres of known $(T_{\rm eff}, [M/H], \log g)$), f_λ^0 is the model spectrum of Vega. Concerning the model atmospheres, we have adopted the homogeneous set of updated ATLAS9 Kurucz model atmospheres and synthetic fluxes (new-ODF models)[2].

3. THE SYNTHETIC IRAC BAND P-L RELATIONS

[1] Available at `http://ssc.spitzer.caltech.edu/irac/`

[2] Available at `http://kurucz.harvard.edu/grids.html` or `http://wwwuser.oat.ts.astro.it/castelli/grids.html`

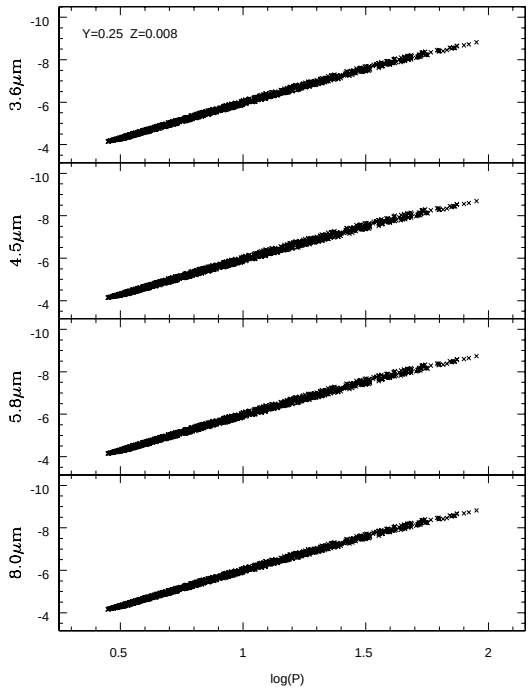


FIG. 1.— Example of the synthetic IRAC band P-L relations, constructed from models with $Y = 0.25$ and $Z = 0.008$.

Figure 1 shows an example of the synthetic IRAC band P-L relations from one of the model sets described in the previous section. All the synthetic P-L relations were fitted with the form of $M_{\rm IRAC} = a + b \times \log(P)$, restricted for pulsators within the period range of $0.4 \leq \log(P) \leq 2.0$ (as in Bono et al. 2010). The fitted P-L slopes (b) and intercepts (a) for each of the models were summarized in Table 1 and 2, respectively. A majority of the model sets do not have pulsators with $\log(P) < 0.4$. For a few of the model sets which have a small number of short-period pulsators, the differences of the P-L slopes and intercepts between the P-L relations derived from full period range and those given in Tables 1 and 2 do not exceed 0.01. In Figure 2, the slopes of the synthetic P-L relations in various bands were compared for six of the pulsating model sets (or chemical compositions), where the linear $BVIJK$ P-L slopes were adopted from Table 2 of Bono et al. (2010)[3]. As expected, the slopes of the P-L relation monotonically decrease from B to K band (see, for example, Madore & Freedman 1991; Berdnikov et al 1996; Caputo et al. 2000; Fiorentino et al. 2002, 2007; Freedman et al. 2008; Ngeow & Kanbur 2008), and "flatten out" in the mid-infrared. However, the 4.5μm P-L relations show a slight increase in their slopes when compared to the "flatter" slopes defined from 3.6μm and 8.0μm band P-L slopes. This slight increase of the 4.5μm P-L slopes, and in some extent to the 5.8μm band P-L slopes, may be explained due to the presence of CO absorption features shown in the $\sim$ 4μm to $\sim$ 6μm spectral region (for further details, see Marengo et al. 2010; Freedman et al. 2011; Scowcroft et al. 2011). In fact, the

[3] For consistency, we only use the linear slopes, b_{all}, from Bono et al. (2010).

slight increase of 4.5μm and 5.8μm band P-L slopes was shown in all model sets presented in Table 1.

4. COMPARISON TO THE EMPIRICAL P-L RELATIONS

Slopes of the current empirical IRAC band P-L relations are summarized in Table 2 of Ngeow & Kanbur (2010). These include six sets of P-L relations in our Galaxy and Magellanic Clouds. Briefly, GAL1 and GAL2 are P-L slopes derived from the "old" and "new" IRSB distances, respectively, and GAL3 are slopes derived from eight Cepheids that possess *Hubble Space Telescope (HST)* parallax measurements. Details concerning these Galactic P-L slopes can be found in Marengo et al. (2010). The LMC1 and LMC2 are the empirical LMC P-L slopes taken from Madore et al. (2009) and Ngeow et al. (2009), respectively, and the SMC P-L slopes were adopted from Ngeow & Kanbur (2010). As discussed in Ngeow & Kanbur (2010), these six sets of P-L slopes can be grouped to two groups characterized by steeper (~ -3.46) and shallower (~ -3.18) slopes respectively. Both of the steeper and shallower slopes can be predicted from using $L_\lambda = 4\pi R^2 B_\lambda(T)$, by assuming the behavior of $B_\lambda(T)$ at long wavelengths for the IRAC bands (see Freedman et al. 2008; Neilson et al. 2010; Ngeow et al. 2010, for more details).

In addition to these six sets of empirical P-L relations obtained from random-phase observations, Scowcroft et al. (2011) have recently published LMC P-L relations based on $\sim$ 80 Cepheids that possess mean magnitudes in 3.6μm and 4.5μm bands. These LMC Cepheids have been observed multiple times using *Spitzer*, with 24 evenly spaced data points per light curves, hence accurate mean magnitudes can be obtained. Their adopted P-L relations in 3.6μm and 4.5μm bands are denoted as LMC3 in this paper.

These empirical P-L relations can be compared to the synthetic IRAC band P-L relations from the selected model sets given in Tables 1 and 2. Bono et al. (2010) have compared the synthetic $BVIJK$ band P-L slopes of these selected model sets to their empirical counterparts for Galactic and Magellanic Clouds Cepheids, and found they are generally in agreement. When comparing the P-L intercepts, three different values of LMC and SMC distance moduli ($\mu_{\rm LMC,SMC}$),[4] respectively, were adopted (see the right panels of Figures 4 and 5). These distance moduli covered a wide range of available distance moduli in the literature for the Magellanic Clouds.

4.1. *Comparison of the Galactic P-L Relations*

A comparison of the synthetic and empirical Galactic P-L relations in IRAC bands are presented in Figure 3. The left panel of this figure shows that the synthetic P-L slopes from $12 + \log(O/H) = 8.58$ ($Z = 0.01$, $Y = 0.26$) and $12 + \log(O/H) = 8.89$ ($Z = 0.02$, $Y = 0.26$) model sets are in marginal agreement with the GAL2 and GAL3 P-L slopes, but not for the GAL1 P-L slopes derived from the "old" IRSB distances. However, the synthetic P-L intercepts from these two model sets agree well with the GAL3 P-L intercepts (albeit the large error bars), but disagree with the other two empirical P-L intercepts based on the IRSB methods. Marengo et al. (2010) have compared the synthetic P-L relations from $12 + \log(O/H) = 8.90$ ($Z = 0.02$, $Y = 0.28$) model set to the three sets of empirical Galactic P-L relations. They are also included in Figure 3. The comparison shown in this figure echoes the finding in Marengo et al. (2010) that this set of synthetic P-L relations agree well with their empirical counterparts derived from the *HST* parallaxes (GAL3), but not for the other two sets of empirical Galactic P-L relations.

Determination of the Galactic P-L relations is expected to improve in the near future. The Carnegie Hubble Program will observe and measure the distances to about 39 Galactic Cepheids in 3.6μm and 4.5μm, with 15 of them expected to have parallax measurements from *Gaia* (Freedman & Madore 2010). The improved empirical Galactic P-L relations are expected to be able to discriminate the synthetic P-L relations that are best at describing the observed P-L relations.

4.2. *Comparison of the LMC P-L Relations*

In Figure 4, synthetic P-L relations from three model sets were compared to the empirical LMC P-L relations. The synthetic P-L slopes from $12 + \log(O/H) = 8.47$ ($Z = 0.008$, $Y = 0.25$) model set are in good agreement with LMC2 P-L slopes from Ngeow et al. (2009). Note that the model set with $Z = 0.008$ and $Y = 0.25$ is generally adopted as a representative metallicity for LMC Cepheids. On the other hand, the synthetic P-L slopes from the $12 + \log(O/H) = 8.35$ ($Z = 0.006$, $Y = 0.25$) model set also agree with LMC1 P-L slopes (from Madore et al. 2009) in 3.6μm and 4.5μm bands, but not in the two longer wavelength bands. Similarly, LMC3 P-L slopes from Scowcroft et al. (2011) agreed with the synthetic P-L slopes from the same model set. For the P-L intercepts, the right panels of Figure 4 show that the synthetic P-L intercepts from $12 + \log(O/H) = 8.35$ model set match with the empirical results from LMC2 if the LMC distance modulus (μ_{LMC}) is adopted to be 18.50 mag. The LMC2 P-L intercepts at 5.8μm and 8.0μm bands also matched to the synthetic P-L intercepts from $12 + \log(O/H) = 8.47$ and $12 + \log(O/H) = 8.17$ model sets if $\mu_{LMC} \sim 18.60$ mag.

The P-L slopes adopted from Scowcroft et al. (2011) are based on Cepheids with period range of $1.0 < \log(P) < 1.8$. Table 3 of Scowcroft et al. (2011) also listed the P-L relations using Cepheids with $0.8 < \log(P) < 1.8$, at which the slopes of these P-L relations (-3.31 ± 0.05 and -3.22 ± 0.05 at 3.6μm and 4.5μm bands, respectively) are in better agreement to the LMC2 empirical P-L slopes from Ngeow et al. (2009) and the synthetic P-L slopes from $Z = 0.004$ and $Z = 0.008$ (both with $Y = 0.25$) model sets given in tje previous section. The synthetic P-L slopes using restricted period ranges, either for $1.0 < \log(P) < 1.8$ or $0.8 < \log(P) < 1.8$, however, do not reproduce the steep slopes as adopted in Scowcroft et al. (2011). In contrast, these P-L slopes are shallower than the synthetic P-L slopes from the full period range ($0.4 < \log[P] < 2.0$). For examples, 3.6μm band P-L slopes for $Z = (0.004,\ 0.006,\ 0.008)$ model sets with $1.0 < \log(P) < 1.8$ are -3.153 ± 0.019, -3.223 ± 0.022 and -3.134 ± 0.017,

[4] Extinction is ignored as it is negligible in IRAC bands (Freedman et al. 2008; Freedman & Madore 2010; Ngeow et al. 2009).

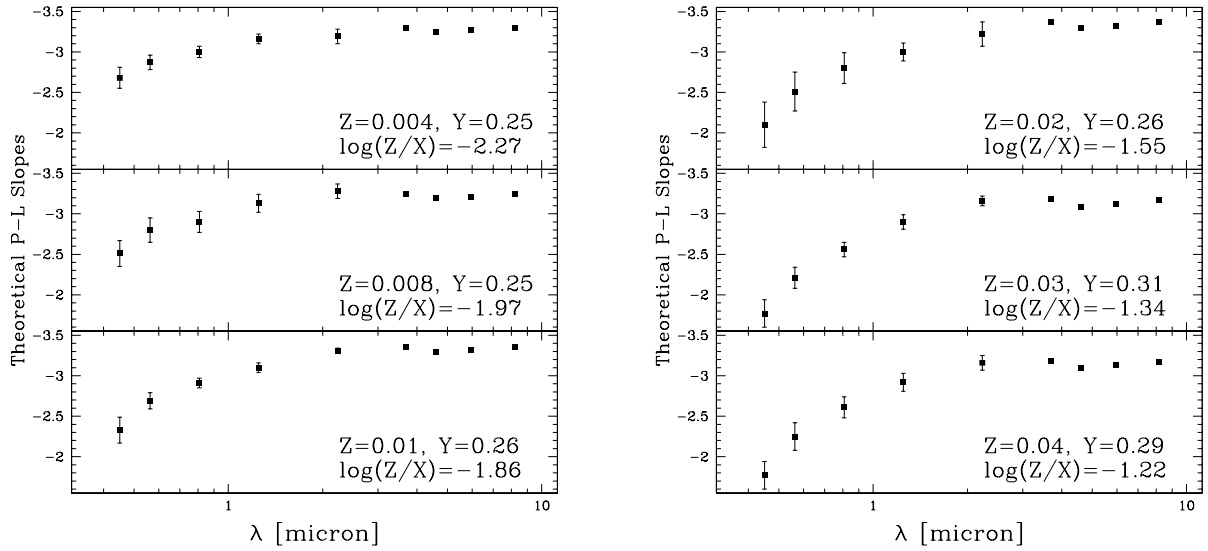


FIG. 2.— Synthetic P-L slopes as a function of wavelength for selected models. Theoretical slopes in $BVIJK$ bands were adopted from Bono et al. (2010, their Table 2).

TABLE 1
SLOPE OF THE THEORETICAL IRAC BAND P-L RELATIONS AT VARIOUS METALLICITIES.

Z	Y	$\log(Z/X)$	$12+\log(O/H)$[a]	[Fe/H][a]	$\Delta Y/\Delta Z$[b]	3.6μm	4.5μm	5.8μm	8.0μm
0.0004	0.24	−3.28	7.16	−1.50	25	-3.511 ± 0.004	-3.506 ± 0.004	-3.513 ± 0.004	-3.519 ± 0.004
0.001	0.24	−2.87	7.56	−1.10	10	-3.344 ± 0.009	-3.323 ± 0.009	-3.336 ± 0.009	-3.352 ± 0.008
0.002	0.24	−2.58	7.86	−0.80	5	-3.510 ± 0.007	-3.485 ± 0.007	-3.498 ± 0.007	-3.517 ± 0.007
0.004	0.25	−2.27	8.17	−0.49	5	-3.292 ± 0.005	-3.253 ± 0.006	-3.269 ± 0.006	-3.298 ± 0.005
0.006	0.25	−2.09	8.35	−0.31	3.3	-3.365 ± 0.007	-3.304 ± 0.008	-3.326 ± 0.008	-3.371 ± 0.007
0.008	0.25	−1.97	8.47	−0.18	2.5	-3.244 ± 0.005	-3.187 ± 0.006	-3.206 ± 0.006	-3.248 ± 0.005
0.01	0.26	−1.86	8.58	−0.08	3	-3.361 ± 0.007	-3.299 ± 0.009	-3.318 ± 0.008	-3.364 ± 0.007
0.02	0.25	−1.56	8.88	+0.22	1	-3.311 ± 0.005	-3.239 ± 0.006	-3.258 ± 0.006	-3.312 ± 0.005
0.02	0.26	−1.56	8.89	+0.23	1.5	-3.369 ± 0.006	-3.304 ± 0.007	-3.322 ± 0.006	-3.372 ± 0.006
0.02	0.28	−1.54	8.90	+0.24	2.5	-3.13 ± 0.01[c]	-3.04 ± 0.01[c]	-3.07 ± 0.01[c]	-3.12 ± 0.01[c]
0.02	0.31	−1.53	8.92	+0.26	4	-3.271 ± 0.005	-3.191 ± 0.005	-3.213 ± 0.005	-3.272 ± 0.005
0.03	0.275	−1.36	9.08	+0.42	1.5	-3.245 ± 0.006	-3.171 ± 0.007	-3.191 ± 0.006	-3.240 ± 0.006
0.03	0.31	−1.34	9.10	+0.44	2.7	-3.179 ± 0.004	-3.093 ± 0.005	-3.118 ± 0.004	-3.167 ± 0.004
0.03	0.335	−1.33	9.12	+0.46	3.5	-3.297 ± 0.003	-3.210 ± 0.004	-3.235 ± 0.004	-3.285 ± 0.004
0.04	0.25	−1.25	9.19	+0.53	0.5	-3.343 ± 0.004	-3.268 ± 0.005	-3.289 ± 0.005	-3.336 ± 0.004
0.04	0.29	−1.22	9.22	+0.56	1.5	-3.182 ± 0.005	-3.104 ± 0.005	-3.125 ± 0.005	-3.172 ± 0.005
0.04	0.33	−1.20	9.25	+0.59	2.5	-3.206 ± 0.002	-3.129 ± 0.003	-3.150 ± 0.002	-3.195 ± 0.002

[a] Calculated from an online tool, `http://astro.wsu.edu/models/calc/MIX.html`, assuming $12+\log(O/H)_\odot = 8.66$.
[b] $\Delta Y/\Delta Z = (Y - Y_p)/Z$ is the relative helium enrichment ratio, where $Y_p = 0.23$ (see Fiorentino et al. 2002, and reference therein).
[c] Taken from Marengo et al. (2010).

respectively. Similarly, the 4.5μm band P-L slopes for $Z = (0.004,\ 0.006,\ 0.008)$ model sets are -3.081 ± 0.022, -3.125 ± 0.025 and -3.046 ± 0.021, respectively. This suggests that the adopted period range could affect the derived P-L relations. Interestingly, Neilson et al. (2010) demonstrated that the empirical P-L slopes based on Ngeow et al. (2009) data can be steepen and consistent to the P-L slopes from Madore et al. (2009), or Scowcroft et al. (2011), if a period cut of $\log(P) = 1.05$ is applied.

4.3. *Comparison of the SMC P-L Relations*

Synthetic P-L relations from three model sets, $12 + \log(O/H) = 7.86$ ($Z = 0.002$, $Y = 0.24$), $12 + \log(O/H) = 8.17$ ($Z = 0.004$, $Y = 0.25$) and $12 + \log(O/H) = 8.47$ ($Z = 0.008$, $Y = 0.25$), were compared to the empirical SMC P-L relations from Ngeow & Kanbur (2010). As can be seen from Figure 5, the synthetic P-L relations from $12 + \log(O/H) = 8.47$ model set agree with the empirical P-L relations, if the assumed SMC distance modulus is 19.10 mag. This result is odd because $Z = 0.004$ is generally adopted as representative of SMC metallicity. Though there is a spread in the metallicity of SMC Cepheids from spectroscopic measurements, the mean value is closer to $Z = 0.004$ than to $Z = 0.008$. This occurrence is due to the fact that current nonlinear pulsation models predict a significant steepening of P-L slopes when changing the metallicity from $Z = 0.008$ to $Z = 0.004$ (with a significant reduction of the dependence at still smaller metal contents) whereas the empirical relations adopted in this paper tend to suggest almost the same slopes for LMC and SMC. For $12 + \log(O/H) = 8.17$ model set, the synthetic P-L slopes agree with the empirical P-L relations

TABLE 2
Intercept of the theoretical IRAC band P-L relations at various metallicities.

Z	Y	$\log(Z/X)$	$12+\log(O/H)$[a]	[Fe/H][a]	$\Delta Y/\Delta Z$[b]	3.6μm	4.5μm	5.8μm	8.0μm
0.0004	0.24	−3.28	7.16	−1.50	25	-2.410 ± 0.004	-2.418 ± 0.004	-2.418 ± 0.004	-2.424 ± 0.004
0.001	0.24	−2.87	7.56	−1.10	10	-2.527 ± 0.010	-2.547 ± 0.011	-2.542 ± 0.010	-2.539 ± 0.010
0.002	0.24	−2.58	7.86	−0.80	5	-2.341 ± 0.006	-2.356 ± 0.006	-2.353 ± 0.006	-2.352 ± 0.006
0.004	0.25	−2.27	8.17	−0.49	5	-2.718 ± 0.005	-2.740 ± 0.006	-2.737 ± 0.006	-2.730 ± 0.005
0.006	0.25	−2.09	8.35	−0.31	3.3	-2.588 ± 0.007	-2.621 ± 0.008	-2.615 ± 0.007	-2.599 ± 0.007
0.008	0.25	−1.97	8.47	−0.18	2.5	-2.702 ± 0.005	-2.724 ± 0.006	-2.723 ± 0.006	-2.714 ± 0.005
0.01	0.26	−1.86	8.58	−0.08	3	-2.577 ± 0.007	-2.594 ± 0.008	-2.595 ± 0.008	-2.590 ± 0.007
0.02	0.25	−1.56	8.88	+0.22	1	-2.608 ± 0.005	-2.609 ± 0.005	-2.617 ± 0.005	-2.621 ± 0.005
0.02	0.26	−1.56	8.89	+0.23	1.5	-2.596 ± 0.005	-2.598 ± 0.006	-2.605 ± 0.006	-2.607 ± 0.005
0.02	0.28	−1.54	8.90	+0.24	2.5	-2.66 ± 0.01[c]	-2.67 ± 0.01[c]	-2.69 ± 0.01[c]	-2.68 ± 0.01[c]
0.02	0.31	−1.53	8.92	+0.26	4	-2.608 ± 0.004	-2.627 ± 0.005	-2.629 ± 0.005	-2.620 ± 0.005
0.03	0.275	−1.36	9.08	+0.42	1.5	-2.630 ± 0.006	-2.619 ± 0.006	-2.629 ± 0.006	-2.647 ± 0.006
0.03	0.31	−1.34	9.10	+0.44	2.7	-2.637 ± 0.004	-2.639 ± 0.005	-2.644 ± 0.004	-2.660 ± 0.004
0.03	0.335	−1.33	9.12	+0.46	3.5	-2.508 ± 0.004	-2.514 ± 0.004	-2.518 ± 0.004	-2.532 ± 0.004
0.04	0.25	−1.25	9.19	+0.53	0.5	-2.545 ± 0.004	-2.525 ± 0.004	-2.537 ± 0.004	-2.563 ± 0.004
0.04	0.29	−1.22	9.22	+0.56	1.5	-2.695 ± 0.004	-2.680 ± 0.005	-2.690 ± 0.005	-2.716 ± 0.004
0.04	0.33	−1.20	9.25	+0.59	2.5	-2.592 ± 0.002	-2.580 ± 0.003	-2.589 ± 0.002	-2.615 ± 0.002

[a] Calculated from an online tool, `http://astro.wsu.edu/models/calc/MIX.html`, assuming $12+\log(O/H)_{\odot} = 8.66$.
[b] $\Delta Y/\Delta Z = (Y - Y_p)/Z$ is the relative helium enrichment ratio, where $Y_p = 0.23$ (see Fiorentino et al. 2002, and reference therein).
[c] Taken from Marengo et al. (2010).

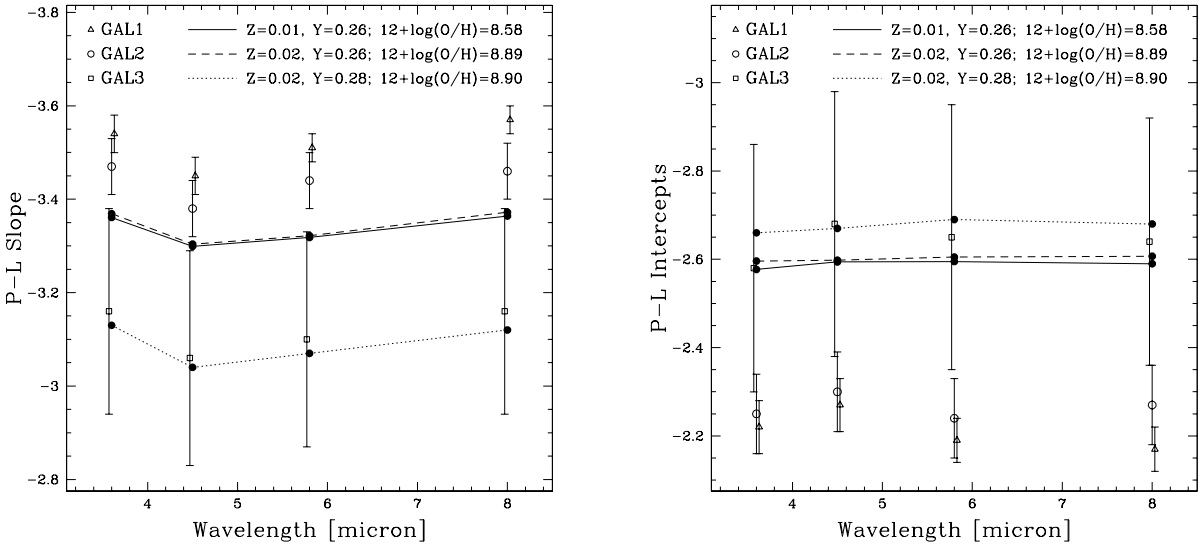


Fig. 3.— Comparison of the empirical Galactic P-L relations, adopted from Marengo et al. (2010), to the selected synthetic P-L relations given in Table 1 (left panel) and 2 (right panel). Note that for better visualization, data points for GAL1 and GAL3 have been shifted slightly in wavelength. See the text for the definition of GAL1, GAL2 and GAL3.

at 5.8μm and 8.0μm bands, though the 3.6μm and 4.5μm P-L slopes are slightly off from the empirical counterparts.

5. DEPENDENCY OF THEORETICAL P-L RELATIONS ON METALLICITY

As mentioned in the Introduction, the IRAC band P-L relations are expected to be insensitive to metallicity. However, based on the residual analysis from multi-band empirical P-L relations for a number of LMC Cepheids with [Fe/H] measurements, Freedman & Madore (2011) suggested the mid-infrared P-L relation could be mildly depending on metallicity. Therefore, possible metallicity dependence of the IRAC band P-L relations is investigated in this section using the synthetic P-L relations presented in Tables 1 and 2. Figure 6 and 7 present the

TABLE 3
F-test results for synthetic P-L relations as a function of metallicity.

Band	P-L Slope	P-L Intercept
3.6μm	15.3	5.68
4.5μm	24.3	3.47
5.8μm	23.3	4.34
8.0μm	17.2	6.46

Note. — We only list the results for $12+\log(O/H)$. The F-test results for [Fe/H] are very similar and hence not listed in this Table.

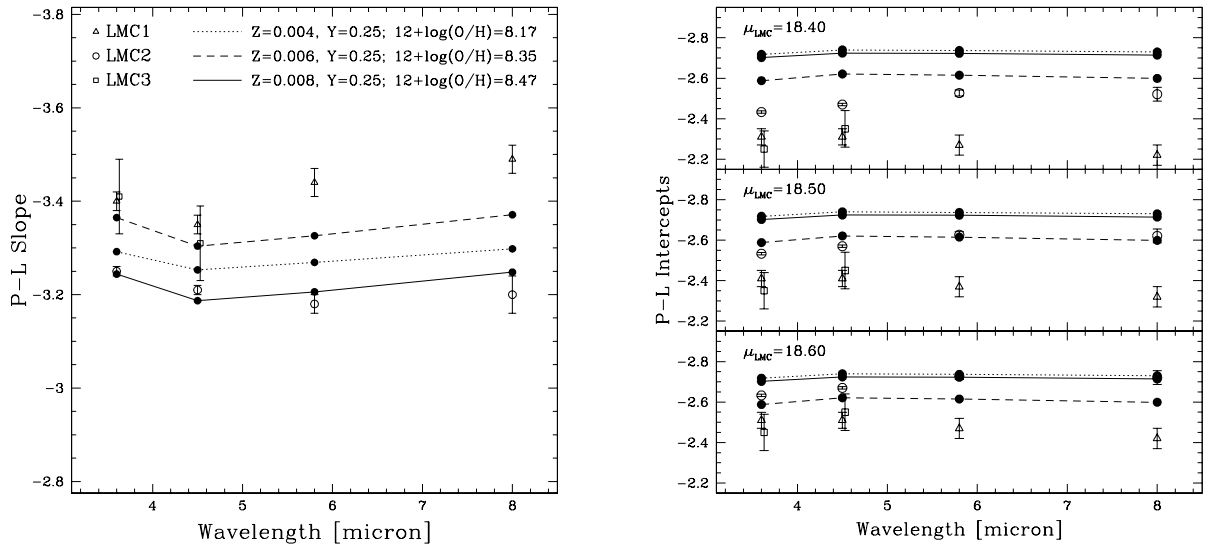


FIG. 4.— Same as Figure 3, assuming three different values of the LMC distance modulus. These distance moduli roughly cover the available LMC distance modulus in literature. Note that for better visualization, data points for LMC3 have been shifted slightly in wavelength.

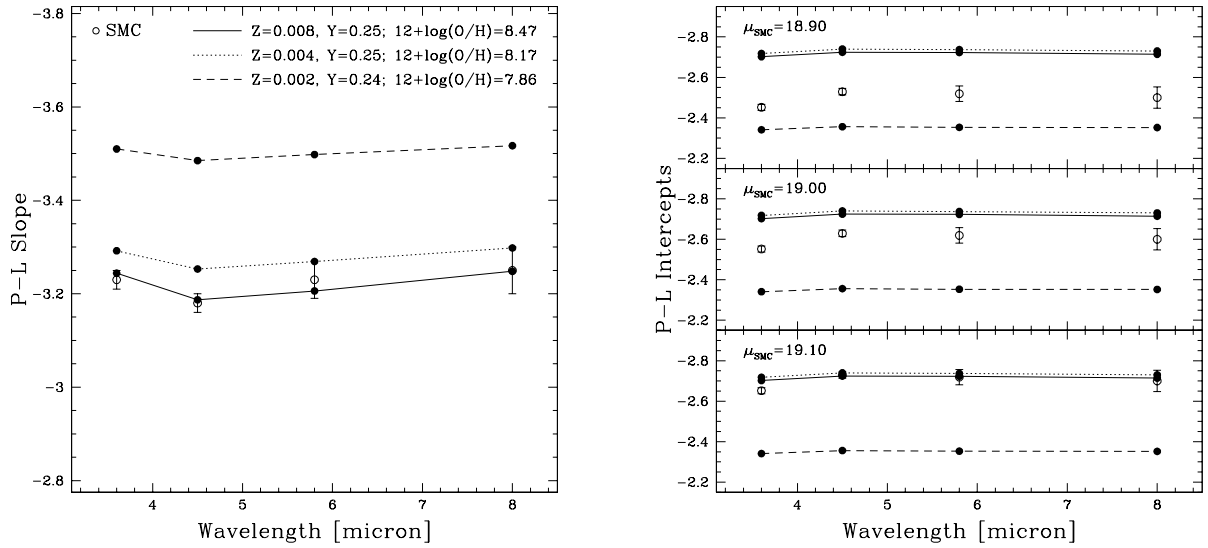


FIG. 5.— Same as Figure 3, assuming three different values of the SMC distance modulus. These distance moduli roughly cover the available SMC distance modulus in literature.

synthetic P-L slopes (left panels) and intercepts (right panels) as a function of $12 + \log(O/H)$[5], suggesting the IRAC band P-L relations may be sensitive to metallicity and/or helium abundance of the Cepheids.

Well known statistical tests can be used to test the possible metallicity dependence of the synthetic P-L relations as shown in Figures 6 and 7. We considered a null hypothesis that the IRAC band P-L relations are independent of metallicity, which can be represented by a constant regression model in the form of $A = a_0$, where A stands for either the P-L slopes or intercepts. The alternate hypothesis is that there is a linear dependency of metallicity on P-L relations represented by a linear regression model, $A = a_0 + a_1 B$ where $B = 12 + \log(O/H)$ or $B = [\mathrm{Fe}/H]$. Graphic representations of these regression models are presented in Figure 8. It is worth to point out that these regression models are used to test the dependency of metallicity on synthetic P-L relations, and do not represent the actual linear dependency of metallicity on P-L relations, since the metallicity effect, if present, will not be a simple linear relation (as evident in Figure 6 and 7). It is well-known in statistical literature (for example, see Kutner et al. 2005) that the F-test can be applied to test if additional parameter (in our case, the a_1) is needed in the regression model. By

[5] Plots for the synthetic P-L relations as a function of $\log(Z/X)$ and $[\mathrm{Fe}/H]$ are similar to these figures, hence omitted from the present paper.

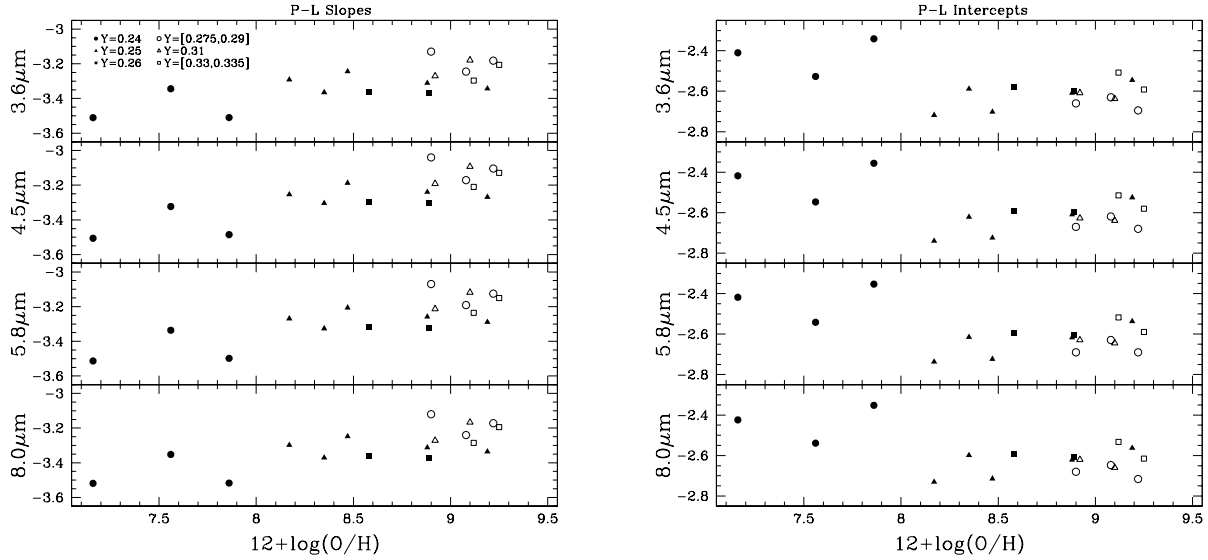


FIG. 6.— Synthetic P-L relations as a function of $12 + \log(O/H)$, separated by the helium abundance (Y). The left and right panels are for the P-L slopes and intercepts, respectively.

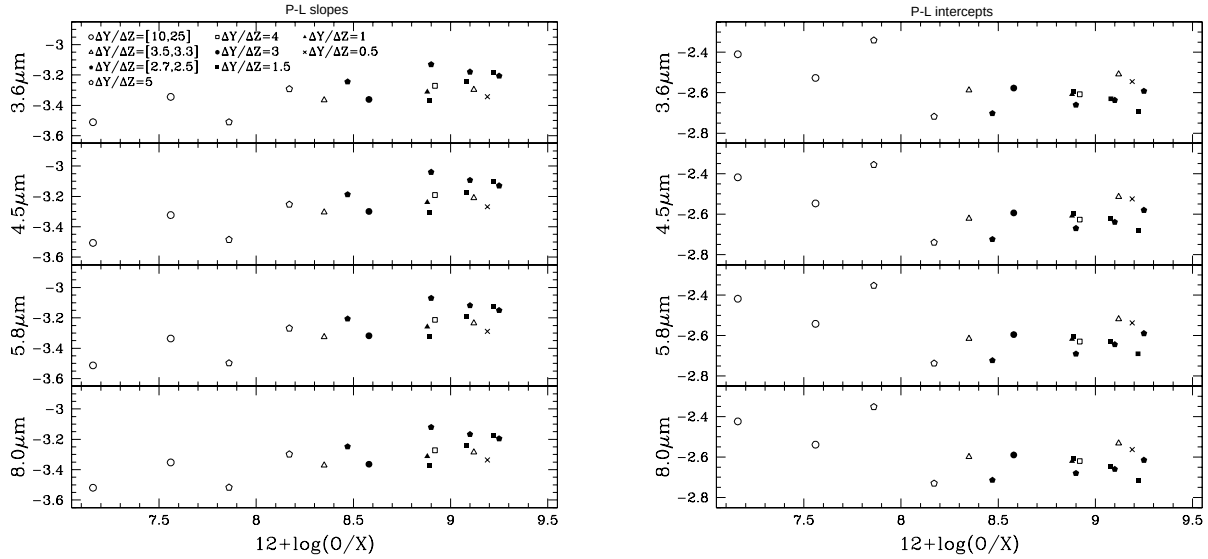


FIG. 7.— Synthetic P-L relations as a function of $12 + \log(O/H)$, separated according to the $\Delta Y/\Delta Z$ values. Note that the open symbols are for $\Delta Y/\Delta Z > 3$, and filled symbols are for $\Delta Y/\Delta Z$ between 1 and 3 (inclusive).

adopting $\alpha = 0.05$, the null hypothesis can be rejected if $F > 4.54$. The F-test results are summarized in Table 3, showing that the null hypothesis can be rejected in most cases, except for 4.5μm and 5.8μm band P-L intercepts. These suggested that the synthetic P-L relations may not be independent of metallicity.

6. THE SYNTHETIC IRAC BAND P-C RELATIONS

Pulsators from various model sets, as described in Section 2, can also be used to construct the synthetic P-C relations in the IRAC bands. For brevity, colors from 3.6μm and 4.5μm bands are denoted as $[3.6]-[4.5]$, and so on. Two examples of the synthetic P-C relations are presented in Figure 9. Results of the synthetic P-C relations are summarized in Table 4. As in the case of the synthetic P-L relations, pulsators with $0.4 \leq \log(P) \leq 2.0$ were used to fit the P-C relations. The P-C slopes and intercepts do not deviate by more than 0.006 if all the pulsators were included. The synthetic P-C slopes and intercepts were plotted as a function of $12 + \log(O/H)$ in Figures 10 and 11, respectively. From these figures, it is clear that P-C relations exist for certain combinations of IRAC band filters and metallicity, and not all of the synthetic P-C relations are independent of metallicity. The P-C relations that are independent or insensitive to metallicity are the $[3.6] - [8.0]$ and $[4.5] - [5.8]$ P-C relations, especially for those with $12 + \log(O/H) < 8.9$.

6.1. *Comparison to Empirical P-C Relations*

Marengo et al. (2010) found a significant $[3.6]-[8.0]$ P-C relation for the Galactic Cepheids, with the expression of $[3.6] - [8.0] = 0.039(\pm 0.008)\log(P) - 0.058(\pm 0.014)$.

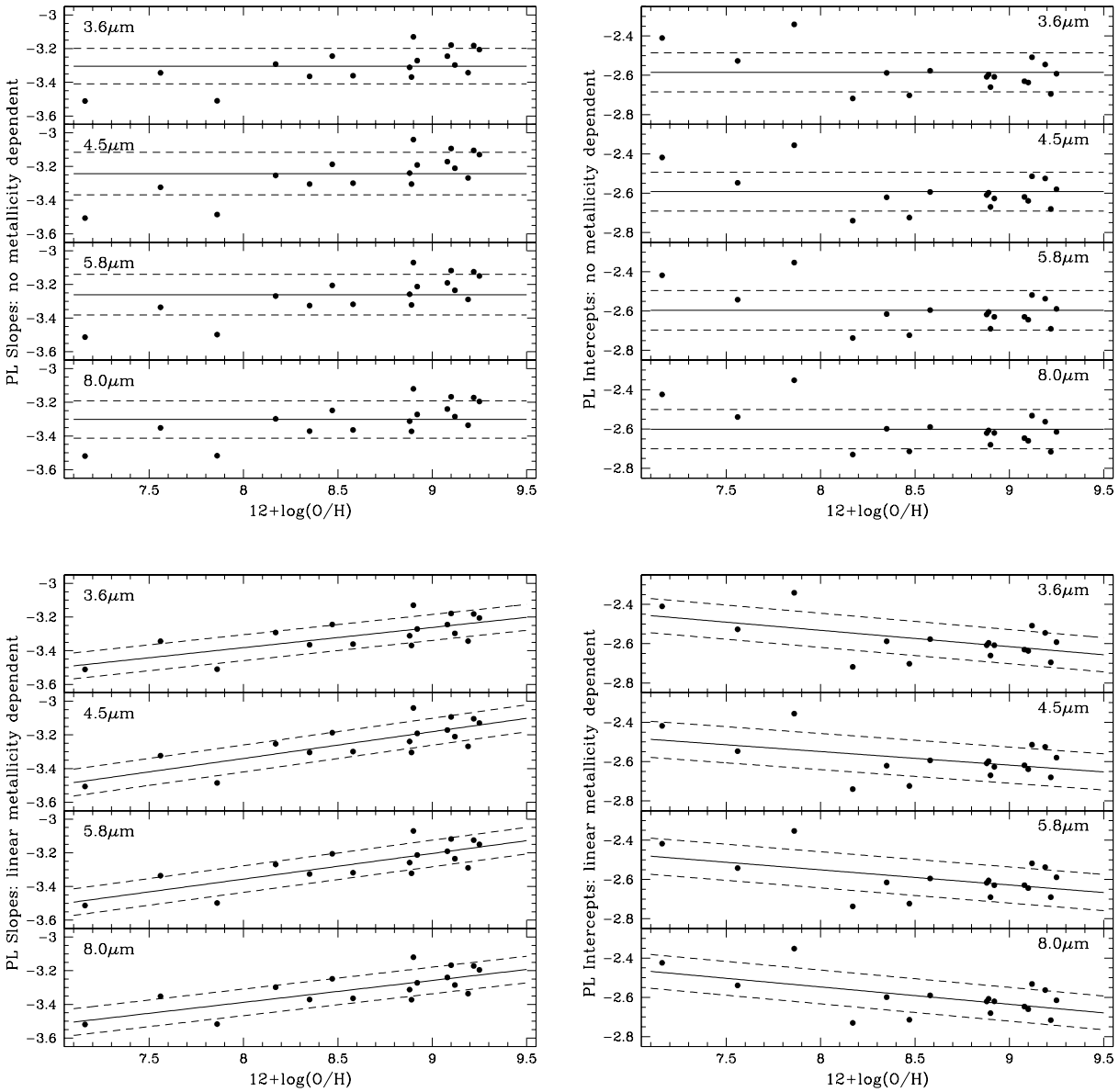


FIG. 8.— Fitting of the constant (upper panels) and linear (lower panels) regression models to the synthetic P-L slopes (left panels) and intercepts (right panels). The dashed lines represent the 1σ boundary of the fitted regressions. The plots for [Fe/H] are very similar to this figure.

This empirical non-zero P-C slope is in contradiction with the synthetic P-C slopes given in Table 4, at which the synthetic $[3.6]-[8.0]$ P-C slopes are close to zero. Disagreement was also found for the P-C intercepts. In Figure 12, P-C relations for 26 fundamental model Galactic Cepheids were compared to the synthetic P-C relations from selected model sets. IRAC band photometry for these Galactic Cepheids were adopted from Marengo et al. (2010). This figure shows that only the $[3.6]-[4.5]$ and $[5.8]-[8.0]$ synthetic P-C relations barely agreed with the observed P-C relations. Disagreements between empirical and synthetic P-C relations may due to the small number of Cepheids in the sample, large photometric errors, colors for all Cepheids are not be measured at mean light, presence of circumstellar envelops especially for longer period Cepheids, uncertainties in the adopted model atmospheres or any combinations of these.

In addition to Galactic Cepheids, Scowcroft et al. (2011) also reported the finding of $[3.6]-[4.5]$ P-C relation based on LMC Cepheids, within the period range of $1.0 < \log(P) < 1.8$, that possess multi-epoch observations. The feft panel of Figure 13 compares the P-C relation for these Cepheids and the three synthetic P-C relations given in Table 4, where the $[3.6]-[4.5]$ colors are obtained from the 3.6μm and 4.5μm band mean magnitudes taken from Scowcroft et al. (2011). It is clear that these synthetic P-C relations do not agree with the empirical P-C relation of $[3.6]-[4.5] = -0.087(\pm0.012)\log(P) + 0.092(\pm0.013)$ from Scowcroft et al. (2011). However, as in Section 4.2, this empirical P-C relation should also be compared to the synthetic P-C relations based on pul-

TABLE 4
Synthetic IRAC band P-C relations at various metallicities[a].

Z	Y	[3.6] − [4.5]	[3.6] − [5.8]	[3.6] − [8.0]	[4.5] − [5.8]	[4.5] − [8.0]	[5.8] − [8.0]
				P-C Slopes			
0.0004	0.24	−0.005	0.002	0.008	0.007	0.012	0.006
0.001	0.24	−0.021	−0.008	0.008	0.013	0.029	0.016
0.002	0.24	−0.024	−0.011	0.008	0.013	0.032	0.019
0.004	0.25	−0.039	−0.023	0.006	0.016	0.045	0.029
0.006	0.25	−0.061	−0.039	0.006	0.023	0.067	0.045
0.008	0.25	−0.057	−0.038	0.004	0.019	0.061	0.042
0.01	0.26	−0.062	−0.043	0.003	0.019	0.065	0.045
0.02	0.25	−0.072	−0.053	0.001	0.019	0.073	0.054
0.02	0.26	−0.065	−0.047	0.003	0.018	0.067	0.050
0.02	0.28	−0.09[b]	−0.06[b]	−0.01[b]	0.03[b]	0.08[b]	0.05[b]
0.02	0.31	−0.079	−0.058	0.001	0.021	0.081	0.059
0.03	0.275	−0.074	−0.054	−0.005	0.020	0.069	0.050
0.03	0.31	−0.086	−0.061	−0.012	0.025	0.074	0.049
0.03	0.335	−0.088	−0.063	−0.012	0.025	0.075	0.051
0.04	0.25	−0.075	−0.055	−0.007	0.020	0.068	0.048
0.04	0.29	−0.078	−0.057	−0.010	0.022	0.068	0.047
0.04	0.33	−0.078	−0.057	−0.011	0.021	0.067	0.045
				P-C Intercepts			
0.0004	0.24	0.008	0.008	0.014	−0.000	0.006	0.006
0.001	0.24	0.020	0.015	0.012	−0.005	−0.008	−0.003
0.002	0.24	0.015	0.012	0.011	−0.003	−0.004	−0.001
0.004	0.25	0.022	0.019	0.012	−0.003	−0.010	−0.007
0.006	0.25	0.034	0.027	0.011	−0.006	−0.023	−0.016
0.008	0.25	0.022	0.021	0.012	−0.001	−0.011	−0.009
0.01	0.26	0.017	0.019	0.013	0.002	−0.004	−0.006
0.02	0.25	0.001	0.008	0.013	0.007	0.012	0.005
0.02	0.26	0.002	0.008	0.011	0.007	0.010	0.003
0.02	0.28	0.01[b]	0.03[b]	0.02[b]	0.02[b]	0.01[b]	−0.01[b]
0.02	0.31	0.019	0.022	0.012	0.002	−0.007	−0.009
0.03	0.275	−0.011	−0.001	0.017	0.010	0.028	0.018
0.03	0.31	0.002	0.006	0.022	0.004	0.021	0.016
0.03	0.335	0.006	0.010	0.023	0.004	0.017	0.013
0.04	0.25	−0.020	−0.009	0.018	0.011	0.038	0.027
0.04	0.29	−0.015	−0.006	0.020	0.010	0.035	0.026
0.04	0.33	−0.012	−0.003	0.022	0.009	0.035	0.026

[a] Errors of the P-C slopes and intercepts are ignored as they are generally less than 0.003.
[b] Derived from the P-L relations.

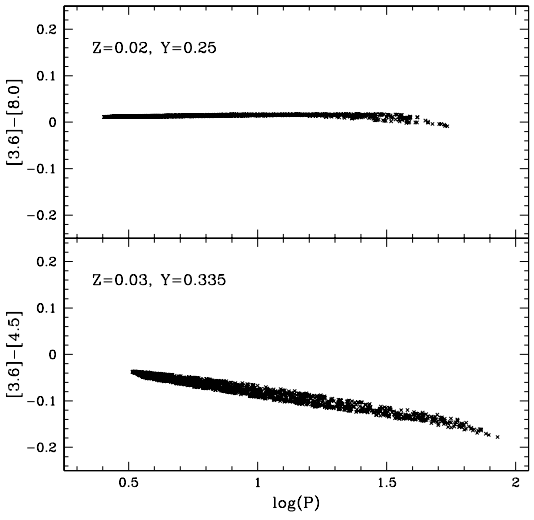


Fig. 9.— Two examples of the synthetic P-C relations in the IRAC band. Top and bottom panels show the example of a flat P-C relation and a P-C relation with largest slope, respectively. The corresponding pulsational model sets are given in the upper-left corners.

TABLE 5
Synthetic [3.6] − [4.5] P-C relation for three models sets with pulsators of $1.0 < \log(P) < 1.8$.

Z	Y	P-C Slope	P-C Intercept
0.004	0.25	-0.072 ± 0.003	0.066 ± 0.004
0.006	0.25	-0.098 ± 0.004	0.082 ± 0.005
0.008	0.25	-0.088 ± 0.004	0.065 ± 0.005

sators within the period range of $1.0 < \log(P) < 1.8$. These synthetic P-C relations for the three model sets are summarized in Table 5, and compared to the empirical P-C relation in the right panel of Figure 13. Table 5 shows that the synthetic P-C slope from ($Z = 0.008$, $Y = 0.25$) model set is in excellent agreement to the empirical P-C slope, although the synthetic P-C intercept is $\sim 2\sigma$ smaller than the empirical counterpart. On the other hand, synthetic P-C relation from ($Z = 0.006$, $Y = 0.25$) model set is also consistent with the empirical P-C relation.

6.2. *The Wesenheit Function*

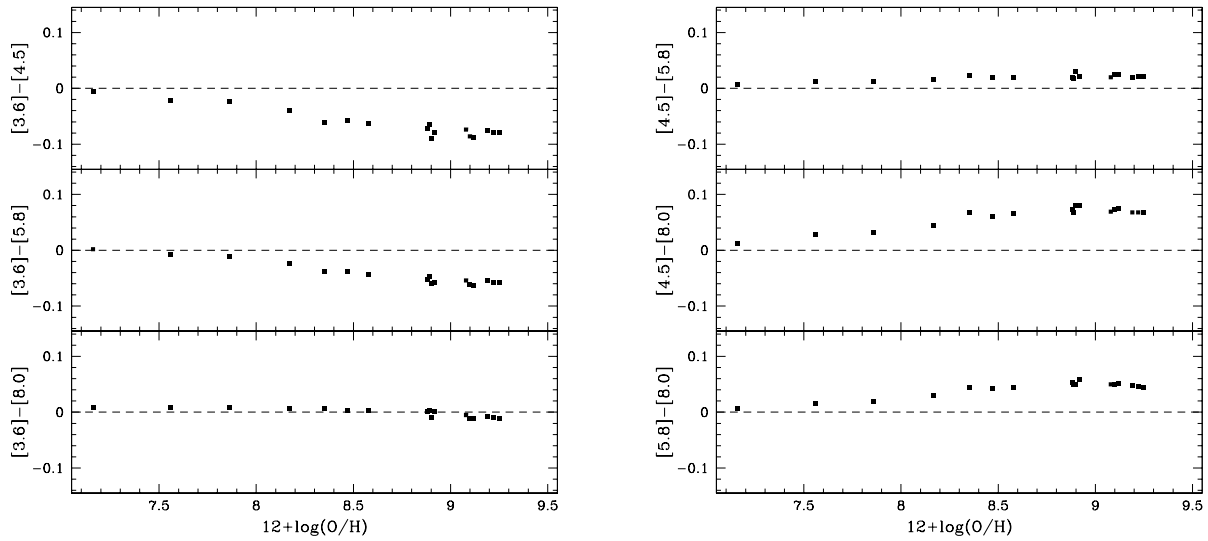


FIG. 10.— Slopes of the synthetic P-C relations as a function of $12 + \log(O/H)$. The dashed lines represent $y = 0$ in order to guide the eyes, and *not* the fitting to the data.

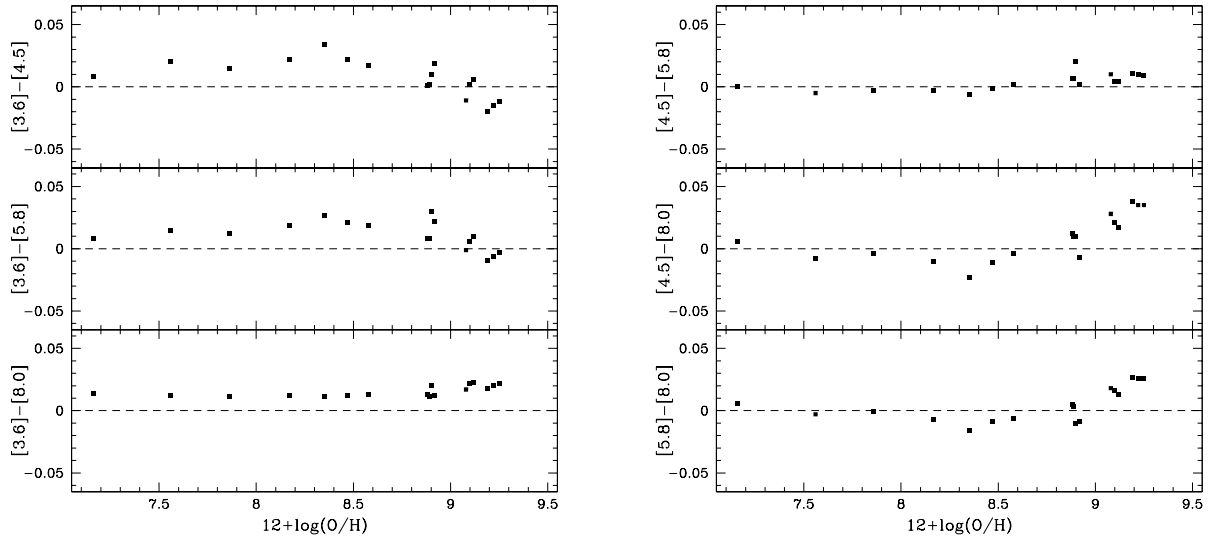


FIG. 11.— Same as Figure 10, but for the intercepts of the synthetic P-C relations.

Existence of the P-C relations suggested the Wesenheit function can be formulated in the IRAC bands. In optical bands, dispersion of the Wesenheit function is ~ 2 to ~ 3 times smaller than the optical P-L relations (for example, see Fouqué et al. 2007; Soszynski et al. 2008; Ngeow et al. 2009, and reference therein). The dispersions of the synthetic Wesenheit function, in the form of $W = m_{3.6\mu\mathrm{m}} - 3.40 \times ([3.6] - [4.5])$, from all model sets are on average about $\sim$ 1.5 larger than the dispersions from the synthetic 3.6μm band P-L relations. Also, it is not worth to derive the IRAC band Wesenheit function because Wesenheit function is reddening-free by definition. On the other hand, extinction can almost be ignored for the IRAC band P-L relations (Freedman et al. 2008; Freedman & Madore 2010; Ngeow et al. 2009; Marengo et al. 2010; Freedman et al. 2011). Therefore, there is no net gain by using the Wesenheit function in the IRAC bands.

7. DISCUSSION AND CONCLUSION

Synthetic IRAC band P-L relations based on a series of pulsation models were investigated in this paper. These synthetic P-L relations were compared to their empirical counterparts, and the possible metallicity dependency of the IRAC band P-L relations was examined. For the former part, selected sets of synthetic IRAC band P-L relations show agreement to the empirical P-L relations derived from Galactic and Magellanic Cloud Cepheids. The $BVIJK$ synthetic P-L relations for these selected model sets also agreed with their optical and near-infrared counterparts, as presented in Bono et al. (2010), for the Galactic and Magellanic Clouds P-L rela-

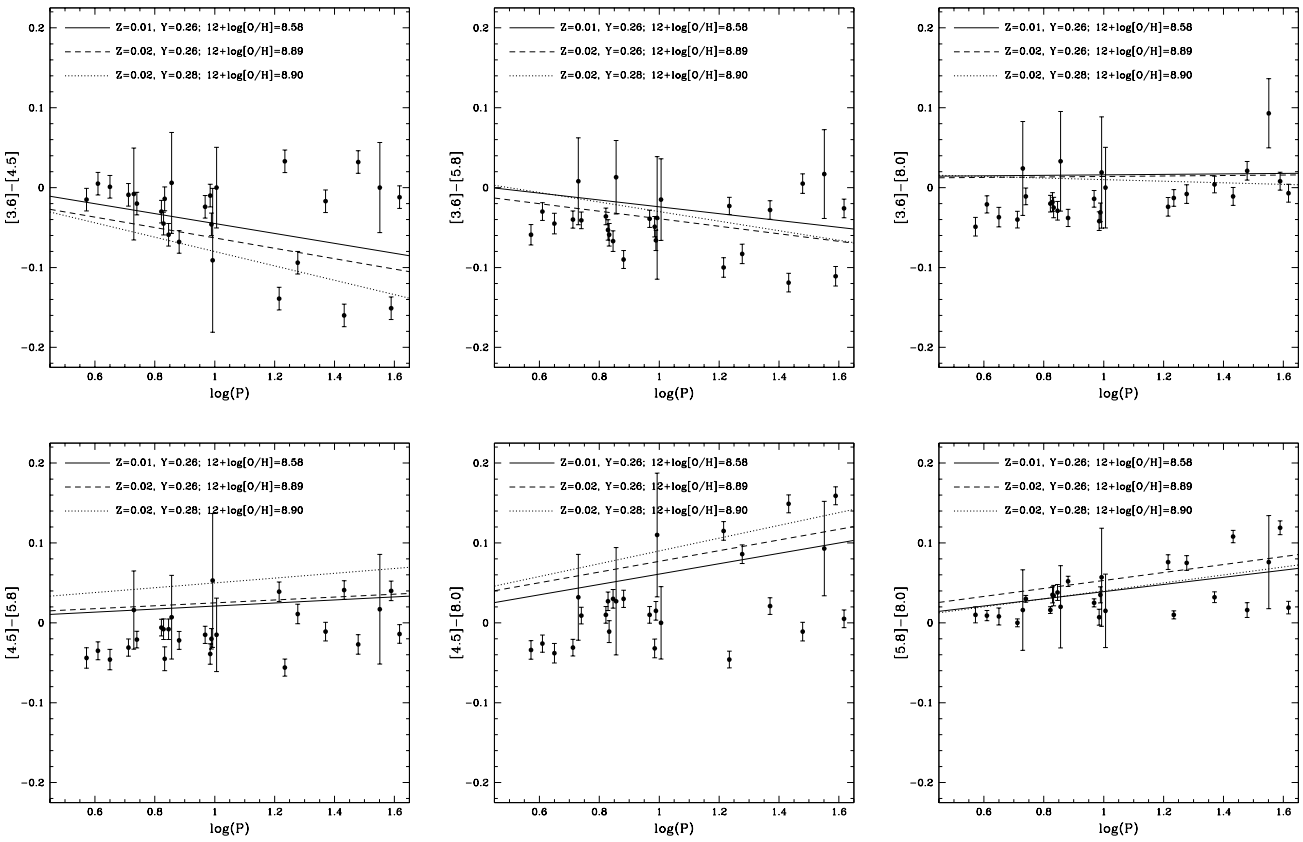


FIG. 12.— Comparison of the P-C relations for Galactic Cepheids and the synthetic P-C relations from three selected model sets given in Table 4. Photometry for Galactic Cepheids is adopted from Marengo et al. (2010).

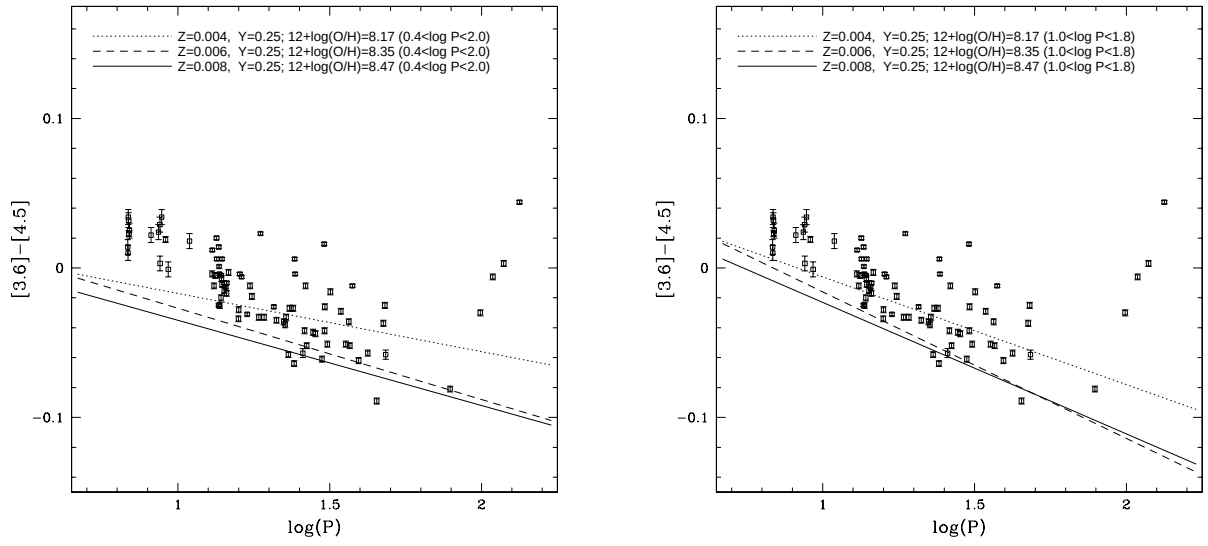


FIG. 13.— Comparison of the P-C relation for LMC Cepheids based on the data presented in Scowcroft et al. (2011) and the synthetic P-C relations from three selected model sets. Left and right panels show the synthetic P-C relations using pulsators in the period range of $0.4 < \log(P) < 2.0$ and $1.0 < \log(P) < 1.8$, respectively.

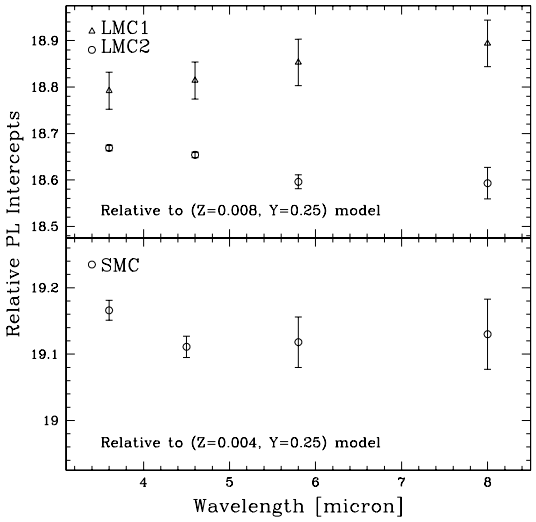


FIG. 14.— Comparison of the P-L intercepts between the empirical P-L relations and the synthetic P-L relations from selected model sets. The top panel shows the comparison for LMC, with synthetic P-L relations selected from ($Z = 0.008$, $Y = 0.25$) model set. The bottom panel shows the comparison for SMC, with synthetic P-L relations selected from ($Z = 0.004$, $Y = 0.25$) model set.

tions. For the metallicity dependency of IRAC band P-L relations, plots for all of the synthetic P-L relations as a function of metallicity revealed that the IRAC band P-L relations may not be independent of metallicity. This result is also supported by statistical F-test. On the other hand, current empirical IRAC band P-L relations based on three galaxies, either the P-L relations in "steep" or "shallow" groups (see Table 2 of Ngeow & Kanbur 2010), suggested the IRAC band P-L relations may not be depending on metallicity, or have a weak dependency on metallicity. It is clear that more empirical determinations of the IRAC band P-L relations are needed, especially for galaxies with low metallicity, from future observations with *JWST*.

Figure 14 shows the intercepts for LMC and SMC empirical P-L relations relative to the two adopted synthetic P-L relations, which is equivalent to derive the distance moduli to the Magellanic Clouds using the synthetic P-L relations. The resulted distance moduli for LMC and SMC are higher than the values commonly adopted in literature (e.g., 18.5 mag and 19.0 mag for LMC and SMC, respectively). This is due to the already mentioned limitation of the adoption of a canonical M-L relation. However, previous theoretical computations of current nonlinear convective models (see, e.g., Bono et al. 2002; Caputo et al. 2002; Bono et al. 2008, and references therein) have shown that by relying on non-canonical models based on an M-L relation brighter than the canonical one by 0.25 dex the inferred distance moduli are shorter than the values obtained in the canonical scenario by 0.15-0.2 mag depending on the filters. This implies that adopting non-canonical relations in the comparison with empirical *Spitzer* data we would have obtained shorter distance moduli by 0.15-0.2 mag for each selected chemical composition, in better agreement with most recent and adopted values in the literature.

Finally, synthetic P-C relations in the IRAC band were also derived and compared to the Galactic and LMC empirical counterparts. In general, disagreements were found between the synthetic and empirical P-C relations. However, the synthetic P-C relations are in agreement with the empirical LMC $[3.6] - [4.5]$ P-C relation if a period range of $1.0 < \log(P) < 1.8$ is adopted when constructing the synthetic P-C relations. Observations of a large number of Cepheids with *JWST* may help in resolving the discrepancy of the IRAC band P-C relations.

The authors thank the referee for constructive comments to improve this manuscript. CCN thanks the funding from National Science Council (of Taiwan) under the contract NSC 98-2112-M-008-013-MY3. This work is based (in part) on observations made with the *Spitzer Space Telescope*, which is operated by the Jet Propulsion Laboratory, California Institute of Technology under a contract with NASA.

REFERENCES

Berdnikov, L. N., Vozyakova, O. V. & Dambis, A. K., 1996, Astronomy Letters, 22, 838
Bono, G., Marconi, M., & Stellingwerf, R. F., 1999, ApJS, 122, 167
Bono, G., Castellani, V., & Marconi, M. 2000, ApJ, 529, 293
Bono, G., Castellani, V., & Marconi, M. 2002, ApJ, 565, L83
Bono, G., Caputo, F., Fiorentino, G., Marconi, M., & Musella, I. 2008, ApJ, 684, 102
Bono, G., Caputo, F., Marconi, M., & Musella, I. 2010, ApJ, 715, 277
Caputo, F., Marconi, M. & Musella, I., 2000, A&A, 354, 610
Caputo, F., Marconi, M., & Musella, I. 2002, ApJ, 566, 833
Caputo, F., Bono, G., Fiorentino, G., Marconi, M., & Musella, I. 2005, ApJ, 629, 1021
Fiorentino, G., Caputo, F., Marconi, M. & Musella, I., 2002, ApJ, 576, 402
Fiorentino, G., Marconi, M., Musella, I., & Caputo, F. 2007, A&A, 476, 863
Fouqué, P., et al., 2007, A&A, 476, 73
Freedman, W. L., Madore, B. F., Rigby, J., Persson, S. E. & Sturch, L., 2008, ApJ, 679, 71
Freedman, W. L. & Madore, B. F., 2010, Annual Reviews of Astronomy and Astrophysics, 48, 673
Freedman, W. L. & Madore, B. F., 2011, ApJ, 734, 46
Freedman, W. L., Madore, B. F., Scowcroft, V., et al. 2011, AJ, 142, 192
Girardi, L., et al., 2002, A&A, 391, 195
Kennicutt, R. C., Jr., et al., 1998, ApJ, 498, 181
Kutner, M., Nachtsheim, C., Neter, J. & Li, W., 2005, Applied Linear Statistical Models (fifth edition), McGraw-Hill, Singapore
Madore, B. & Freedman, W., 1991, PASP, 103, 933
Madore, B. F., Freedman, W. L., Rigby, J., Persson, S. E., Sturch, L. & Mager, V., 2009, ApJ, 695, 988
Marconi, M., Musella, I., & Fiorentino, G., 2005, ApJ, 632, 590
Marconi, M., et al., 2010, ApJ, 713, 615
Marengo, M., Evans, N. R., Barmby, P., Bono, G., Welch, D. L. & Romaniello, M., 2010, ApJ, 709, 120
Neilson, H. R., Ngeow, C.-C., Kanbur, S. M., & Lester, J. B. 2010, ApJ, 716, 1136
Ngeow, C.-C. & Kanbur, S. M., 2008, ApJ, 679, 76
Ngeow, C.-C., Kanbur, S. M., Neilson, H. R., Nanthakumar, A. & Buonaccorsi, J., 2009, ApJ, 693, 691
Ngeow, C.-C. & Kanbur, S. M., 2010, ApJ, 720, 626
Ngeow, C.-C., Ita, Y., Kanbur, S. M., Neilson, H., Onaka, T. & Kato, D., 2010, MNRAS, 408, 983

Scowcroft, V., Freedman, W., Madore, B. F., Monson, A. J., Persson, S. E., Seibert, M., Rigby, J. R., & Sturch, L. 2011, ApJ In-press (arXiv:1108.4672)

Soszynski, I., et al., 2008, Acta Astron., 58, 163